INTERNATIONAL ATOMIC ENERGY AGENCY
UNITED NATIONS EDUCATIONAL, SCIENTIFIC AND CULTURAL ORGANIZATION

INTERNATIONAL CENTRE FOR THEORETICAL PHYSICS
34100 TRIESTE (ITALY) - P.O.B. 586 - MIRAMARE - STRADA COSTIERA 11 - TELEPHONES: 224281/2/3/4/5/6
CABLE: CENTRATOM - TELEX 460392-1

SMR/115 - 19

WINTER COLLEGE ON LASERS, ATOMIC AND MOLECULAR PHYSICS

(21 January - 22 March 1985)

UV AND VUV LASERS

F.P. SCHAEFER
Max-Planck-Institut für Biophysikalische Chemie
Abteilung Laserphysik
3400 Göttingen-Nikolausberg
Fed. Rep. Germany

Winter College on Lasers, Atomic and Molecular Physics,
Miramare-Trieste, Italy; 21 January - 22 March 1985

UV and VUV Lasers

Fritz P. Schäfer
Max-Planck-Institut für biophysikalische Chemie, Abteilung
Laserphysik, D-3400 Göttingen, Fed. Rep. Germany

Introductory Remarks

These lecture notes will only treat fundamental frequency generation in the UV and VUV to XUV region by lasers which are at present or promise to become in the future the work horses for applications in fundamental and applied science as well as in industry. This excludes generation of coherent optical radiation in this spectral region by nonlinear optical techniques, as e.g. frequency-multiplication or Raman-shifting of visible or NIR lasers, as well as discussion of lasers with intrinsic or technical limitations, as e.g. hollow-cathode lasers. At present this leaves us with excimer lasers (actually only a few of the many possible types) and lasers pumped by a laser-generated plasma. Thus, the first lecture will concentrate on excimer lasers, the second on so-called "X-ray lasers". It is clear that in the short time available only the principles, some typical examples, and some remarks on developmental trends can be given, while an exhaustive treatment of the extensive literature in either case would require a full semester's course. Enough literature references will be cited for a detailed study of all topics.

I. Excimer Lasers (1)

1. Excimers and Exciplexes

It has become standard practice, to call all molecules that can only exist in an excited state "excimers" (originally derived from "excited dimer"). This includes e.g. homonuclear dimers of the noble gases, like He_2^*, Ar_2^* etc., as well as mixed noble gas dimers as $ArXe^*$. Other molecules that should strictly be called "exciplexes" (for "excited complex"), are the noble-gas halides, e.g. $XeCl^*$, ArF^* etc., the noble-gas oxides, e.g. XeO^*, or triatomic molecules as Ar_2F^*. The term excimer is often even applied to stable compounds like the halogen molecules, e.g. F_2, or interhalogen compounds, e.g. IF, since they possess excited states that resemble closely in their spectroscopic properties the true excimers and behave similarly in laser devices. Many of these "excimers" emit in the visible and near UV. Even of those which emit in the UV and VUV only a few are useful for powerful lasers. These are in the order of decreasing laser wavelength XeF^* at 352 nm, $XeCl^*$ at 308 nm, KrF^* at 248 nm, ArF^* at 193 nm, Xe_2^* at 172 nm, and F_2 at 158 nm.

2. Spectroscopic Properties

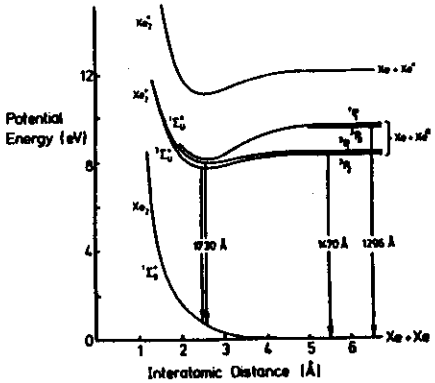

Fig. 1

The potential energy curves of Xe_2 are shown in Fig 1. An excited and a ground state Xe-atom colliding can be seen to be able to form a stable compound, provided the excess vibrational and rotational energy can be dissipated in collisions with other atoms or the walls. This is due to a covalent bond formed between the two atoms. The radiative transitions from the singlet or triplet excited states to the repulsive ground state have strong transition moments, which also means relatively short radiative lifetimes of about 100 ns and high cross-sections for stimulated emission.

Typical potential energy curves for rare-gas halides MX are shown in Fig. 2, where M is the rare-gas and X the halogen.

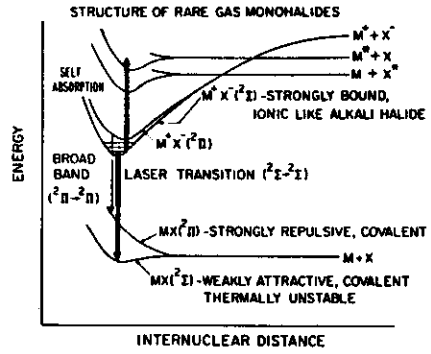

Fig. 2

Here one sees that a rare-gas ion M^+ and a halogen ion X^- can form a strongly bound excimer by an ionic bond as in an alkali halide. The bond can either be a σ- or a π-bond, so that we have a lowest $^2\Sigma$-state, usually referred to as the B-state, and a slightly more energetic $^2\Pi$-state, usually referred to as the C-state. One also notes that the potential energy curves of an excited rare-gas atom and a ground-state halogen atom or an excited halogen atom colliding with a ground-state rare-gas atom cross the curve of the ion pair, so that by diabatic curve crossings these systems will also finally populate the B- and C-states. The ground states are a strongly repulsive covalent $^2\Pi$-state, usually called the A-state, and a weakly attractive but thermally unstable $^2\Sigma$-state, called X-state. The transition B→X normally has a very strong transition moment, whereas the C→A transition is weak and very broadband. The normally used laser transition in

excimer lasers is the B→X transition, even though widely tunable but weak excimer lasers have recently been operated on C→A transitions, when the B→X transition was artificially suppressed. The radiative lifetimes are as follows: XeF ≈ 15 ns, XeCl = 11 ns, KrF = 6.8 ns, ArF = 4.2 ns. The oscillator strength of these allowed charge transfer transitions is about unity, as in dye lasers, but line widths are smaller, so it is clear that high gain is to be expected in rare-gas halide excimer lasers even at relatively low concentrations. Figure 3 shows the fluorescence spectrum of KrF with the B→X and the C→A transitions and that of the trimer Kr_2F that becomes more prominent at higher pressures.

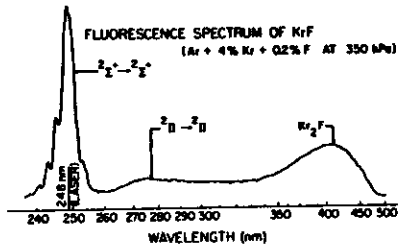

Fig. 3

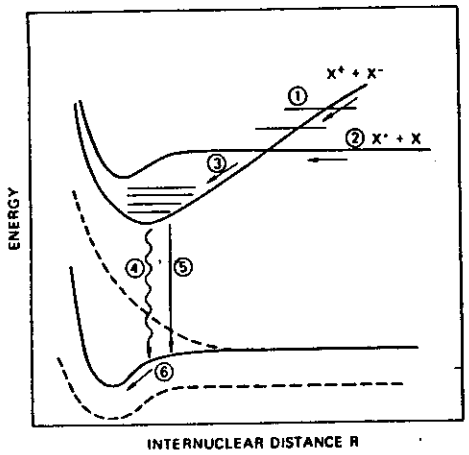

Fig. 4

Figure 4 schematically shows the potential energy curves of a halogen molecule, like F_2. Again the lowest upper state is ionic in character and the lower state is covalently bound, thus resembling the rare-gas halide excimers. Since we here have a bound-bound

transition, maintenance of an inversion depends on rapid vibrational relaxation and possibly other processes, like predissociation.

3. Electron-Beam-Pumped Excimer Lasers

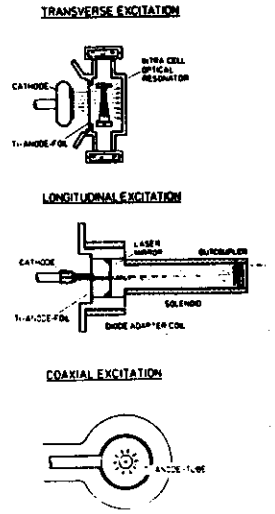

Fig. 5

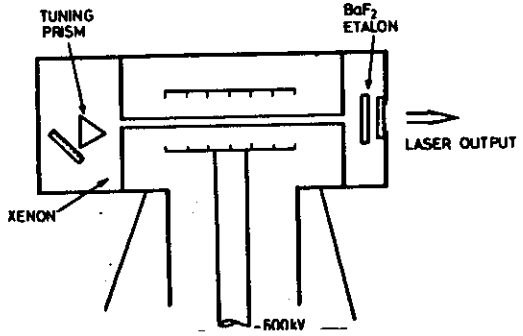

Fig. 6

Figures 5 and 6 show some experimental arrangements with transverse (2), longitudinal (3) and coaxial (4) pumping. The very low repetition rates, relatively low efficiency, and high cost of the e-beam machines have made this method of pumping almost obsolete for practical purposes, even though for very high pulse energies and for fundamental studies they are still valuable.

Xe_2^*-LASER MECHANISM

$Xe + e = Xe^* + e$	e-beam pumping
$Xe^* + Xe = Xe_2^*$	excimer formation
$Xe_2^* + h\nu = Xe + Xe + 2h\nu$	laser gain
$Xe_2^* + h\nu = Xe_2^{**} + e$	reabsorption
$Xe_2^* + Xe = Xe + Xe + Xe$	loss
$Xe_2^* + Xe_2^* = Xe_2^{**} + Xe + Xe + e$	loss

Figure 7 gives a listing of the most important elementary steps of an e-beam-pumped Xe_2^*-laser. (This laser could not yet be pumped by pure discharges.)

Fig. 7

Similar, however more complicated, sets of elementary steps must be used in order to describe the behavior of rare-gas halide lasers. This is a consequence of the three or more components gas mixtures used in these lasers. A typical example is the mixture used in a KrF laser consisting of 5 % Kr, 0.2 % F_2, and the rest Ar with total pressures of 2 to 10 atm. The rare-gas atoms in an excited state after an electron collision forms an excimer in a "harpooning" reaction with ground-state halogen molecules:

$$Kr^* + F_2 \rightarrow KrF^* + F.$$

Instead of excited atoms, excimers can also be formed from ions, predominantly by

$$e^- + F_2 \rightarrow F^- + F \text{ and } F^- + K^+ + Ar \rightarrow KrF^* + Ar.$$

Apart from quenching collisions, like

$$e^- + KrF^* \rightarrow Kr + F + e^- \text{ (superelastic collisions)},$$

the main loss terms arise from photoabsorption:

$F_2 + h\nu \rightarrow 2F$	(photodissociation)
$F^- + h\nu \rightarrow F + e^-$	(photodetachment)
$Ar^* + h\nu \rightarrow Ar^+ + e^-$ $Ar_2^* + h\nu \rightarrow Ar_2^+ + e^-$	(photoionization)
$Ar_2^+ + h\nu \rightarrow Ar^+ + Ar$	(photodissociation)

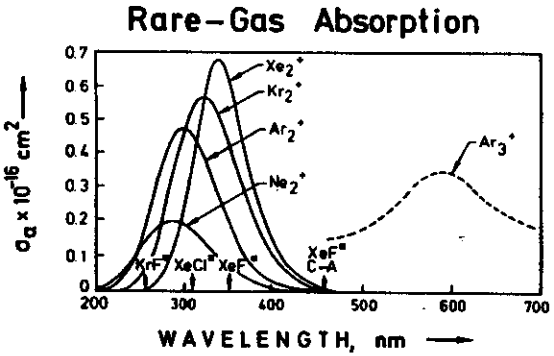

Fig. 8

Figure 8 shows some relevant absorption spectra for halogens. Some of these losses can be avoided by using halogen donors that do not absorb in the region of the laser wavelength, e.g. HCl in XeCl lasers instead of Cl_2, and NF_3 instead of F_2 in KrF lasers. Often, however, performance of these lasers is reduced by unfavorable kinetics and side-reactions of the halogen donors.

4. Discharge-Pumping

The formation of excited atoms and of ions by electron collisions can, of course, also occur in electrical discharges through the appropriate gas mixtures. The difficulty is that these discharges, which should occur simultaneously and homogeneously between two elongated electrodes, are intrinsically unstable, forming arcs and sparks after some time after initiating the discharge. In addition, it is difficult to match a constant impedance power supply to a discharge that starts from a very high impedance and finally ends with a very low impedance of often no more than a fraction of one Ohm.

For this reason one has to use some means for providing a relatively uniform level of ion density in the mixture, before power is applied to the electrodes. The first method is a natural extension of e-beam pumping, namely applying some preionization by an e-beam, as shown in Fig. 9.

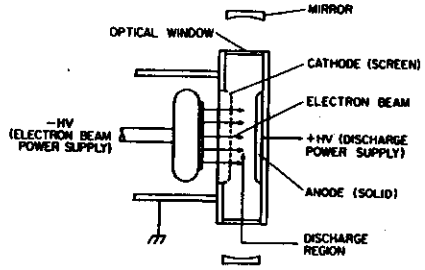

Fig. 9

The second method makes use of a series of small sparks not far from the main electrodes, whose hard UV-radiation ionize impurities of low ionization potential in the gas mixture and

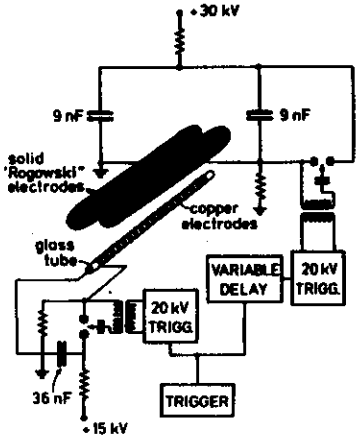

thus supply the necessary preionization level (5). These sparks must be created some 100 ns to 1 µs before the main discharge is switched on, so that the charge carriers can be uniformly distributed by diffusion. An example of an excimer laser using this method is shown in Fig. 10.

Fig. 10

The third and most recent method, which has by far the highest potential for high power, high efficiency excimer lasers is X-ray preionization. In this case an X-ray flashtube using either a cold or heated line-shaped cathode and a pulsed voltage of 50 to 300 kV is fired just before or simultaneous with the switching-on of the voltage to the main discharge electrodes, so that the whole volume of the gas mixture between the electrodes is very uniformly ionized even at very high gas pressures. In contrast to UV-preionization which can only be used for gaps of a few centimeters, X-ray preionization has been used for the preionization of discharge volumes of several cubicmeters. Figure 11 shows just one of the many possible realizations of this method.

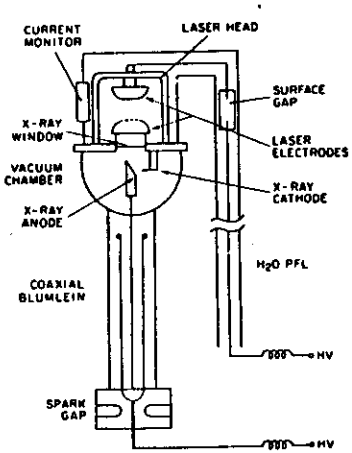

Fig. 12

5. Power Supplies and Switching

The two main problems that plague excimer laser designers are 1. energy storage and conduction to the main electrodes with extremely low impedance for matching the impedance of the fully developed discharge and 2. high-current, high-voltage switching of the main discharge. These are determined by the necessary E/p-ratios for a fully developed discharge, which in most rare-gas halogen lasers is found to be approximately 2.5 $kV \cdot cm^{-1} \cdot atm^{-1}$. This means that actually for a gap of 3 cm and a pressure of 2 atm a voltage of 15 kV should suffice. In practice about twice that value is necessary because of the inductivity of the conductors connecting electrodes and energy storage and because of dissipative and inductive losses in the switching means. As energy storage means either low-inductance capacitors or transmission lines are used. The latter usually take the form of solid-state transmission lines, mostly for smaller lasers, or water Blümlein transmission lines for high pulse energies (7).

The high-current, high-voltage switches presently used in most commercial excimer lasers up to pulse energies of about 1 J are specially adapted thyratrons. For larger pulse energies at present the only possibility are spark gaps, especially in the form of so-called rail-gaps. A promising recent development are light-activated silicon switches (8), which are intrinsically reliable and simple, but unfortunately need another laser as light source for switching. Another recent development is the so-called magnetic switching (9), which actually means the introduction of a saturable inductivity between the electrodes and the thyratron. If the core of this inductor is made of a material with a nearly rectangular hysteresis loop (e.g. special ferrites or amorphous metals) then the transition from high unsaturated to low saturated inductivity is

very abrupt with a concomitant fast current rise. This relaxes the dI/dt-demand on the thyratron with a corresponding increase in reliability and life of the thyratron.

6. Materials Considerations

In rare-gas halide lasers the presence of aggressive halogens or halogen compounds necessitates the use of materials for the construction of such lasers, which are fully compatible with halogens. The worst halogen in this respect is certainly fluorine. The best material for the frame work and enclosure of excimer lasers was found to be polyvinylidenfluoride (PVDF). As electrode material nickel-plated stainless steel has the best overall properties. After some passivation for some hours in an atmosphere with high fluorine content, the nickelfluoride coating is quite stable. Nevertheless, some almost unavoidable arcing at the end of the pulse discharge causes some sputtering. The sputtered material is introduced into the gas circulation as a fine powder which deposits a scattering film almost everywhere, e.g. also on the windows which can mean a serious reduction in output energy. This can be avoided by introduction of filters in the gas circulation system and a careful design of the flow pattern of the circulating gas. The unavoidable chemical reactions that use up the halogen can be compensated for by an appropriate gradual admixture of additional halogen. The impurities that would gradually pile up in the gas as a consequence of these chemical reactions have a lower vapour pressure than the noble gases and halogens and thus can be trapped in a cold trap of suitably adjusted temperature in the gas circulation path. All these processes as well as the capacitor charging voltage can be controlled by a microprocessor so that a constant output pulse energy can be maintained in modern commercial excimer lasers for many millions of shots, in contrast to a few tens of shots in early laboratory lasers, before there is a need for a new gas filling (10).

7. Developmental Trends

At present commercial excimer lasers operate with pulse energies of up to one Joule and pulse repetition rates of up to 1 kHz, although both conditions cannot be fulfilled simultaneously. Nevertheless, average output powers of more than 100 W have been achieved and more than 1 kW can be expected in the near future.

The recent introduction of X-ray preionization has allowed the use of very large apertures, e.g. 1 m x 1 m in a KrF laser developed in Los Alamos National Laboratories, which has already delivered pulse energies of more than 5 kJ. In Japan a very large KrF laser is under construction that is designed for 1 MJ pulse energies. The incredible scalability of excimer lasers is demonstrated by the fact that even lasers for 1 MJ and 100 MJ have been seriously considered for laser fusion work. While most of these devices have been used with pulse lengths of a few nanoseconds, it has recently been demonstrated that excimer lasers can also be used with high efficiencies for amplification of pulses as short as 2 ps to powers of 20 GW (11), and probably very soon pulses of terawatt peak power with only 150 fs duration (as determined by the spectral bandwidth of the B→X excimer transitions in XeCl and KrF) will be demonstrated. We can thus foresee a wealth of exciting new developments and applications of excimer lasers.

References

1. Excimer Lasers, Ch. K. Rhodes, Ed., Second Enlarged Edition, Springer-Verlag, Berlin etc., 1984
2. F. K. Tittel, J. Liegel, W. L. Wilson, Jr., G. Zhenhua, G. Marowsky: Tuning characteristics of broadband excimer lasers. - Proc. Int. Conf. Lasers '81, New Orleans, USA, Dec. 14-18, 1981, Ed. C. B. Collins, STS Press, McLean, VA, 1982; pp 8 - 14.
3. See Ref. 2
4. D. J. Bradley, D. R. Hull, M. H. R. Hutchinson, M. W. McGeoch: Opt. Commun. 11 (1974) 335
5. R. Burnham, N. Djeu: Appl. Phys. Lett. 29 (1976) 707
6. K. Midorikawa, M. Obara, T. Fujioka: IEEE J. Quant. Electron. QE-20 (1984) 198
7. L. F. Champagne, A. J. Dudas, B. L. Wexler: "Progress on the scaling of the x-ray preionized discharge-pumped XeCl laser", Excimer Lasers, Their Application and New Frontiers in Lasers, R. W. Waynant, Editor, Proc. SPIE 476, p 2 - 5
8. O. S. F. Zucker, J. R. Long, V. L. Smith: Appl. Phys. Lett. 29 (1976) 261
9. I. Smilanski, S. R. Byron, T. R. Burkes: Appl. Phys. Lett. 40 (1982) 547
   and: D. Basting, K. Hohla, E. Albers, H. v. Bergmann: Laser und Optoelektronik, No. 2, 1984, pp 128 - 131 (in English)
10. See enclosed manufacturer's information.
11. P. B. Corkum, R. S. Taylor: IEEE J. Quant. Electron. QE-18 (1982) 1962
    and enclosed reprint

II. X-ray Lasers

1. Why X-ray Lasers

Apart from the drive of fundamental research to demonstrate the feasability of X-ray lasers, there are many practical reasons to develop X-ray lasers. Foremost among them rank microscopy and microlithography (1). (We will not discuss here any weapons applications of "Star Wars" fame.) For biological X-ray microscopy the spectral region of 2.3 to 4.4 nm is of special importance since there the absorption coefficient of water and protein differ by one order of magnitude, allowing microscopy of unstained living cells of up to 1 µm thickness with high contrast and resolution. Presently such work has to be done with synchrotron radiation, which is very time-consuming and cost-intensive. An X-ray laser of suitable wavelength would allow a much more wide-spread application of this method. The same can be said of sub-micron lithography for semiconductor-chip production. Finally, X-ray lasers would allow holographic applications with extremely high resolution e.g. in crystallography.

2. Elementary Facts of X-Ray Physics - a Brief Reminder

The usual definition of the spectral region of X-rays is from 0.1 to 10 Å, corresponding to quantum energies of 1 to 100 keV, but these boundaries are rather fuzzy. The two mechanisms for the generation of X-ray radiation are

a) Bremsstrahlung, which is caused by the scattering of electrons in matter (Fig. 1) creating a continuous spectrum (Fig. 2);
b) electron jumps between inner shells of atoms, creating the so-called characteristic line radiation (Fig. 3).

Fig. 1

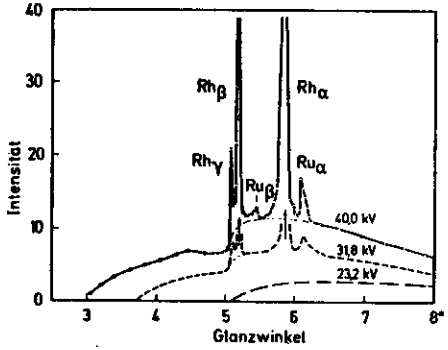

Fig. 3

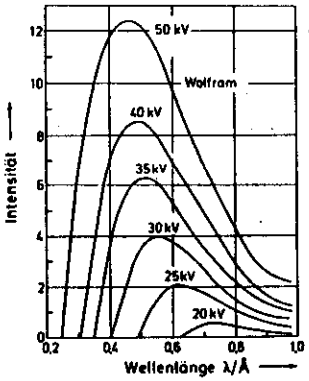

Fig. 2

For X-ray lasers only the second process is of importance. For this process to occur one must at first create a vacancy in an inner shell by ionizing electron collision or absorption of sufficiently hard X-ray radiation. A vacancy created e.g. in the K-shell will be filled by electron jumps from the L, M, N, ... shells thus creating the K_α, K_β, K_γ, ... lines. Similarly, the L_α,

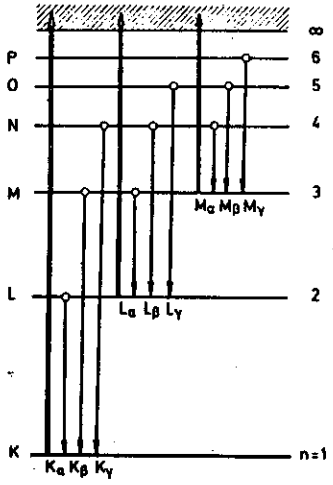

Fig. 4

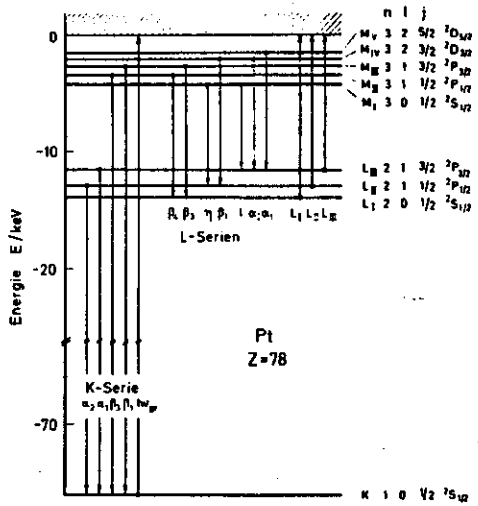

Fig. 5

L_β, L_γ, ... lines are created by filling in a vacancy in the L shell etc., as indicated in Fig. 4. For an explanation of the fine structure of the line spectra one has to consider, in addition to the main quantum numbers, also the orbital and spin quantum numbers, as shown in Fig. 5.

The absorption spectra of atoms in the X-ray region are essentially continuous spectra since they are created by electronic transitions from an inner shell into the continuum beyond the ionization potential. The absorption coefficient for such a transition decreases with increasing energy, until the ionization limit of the next lower lying shell is reached, so that at any wavelength the absorption coefficient is a sum of contributions from the transitions from various shells. This has the important consequence for optically pumping X-ray lasers that a wavelength beyond, say, the K-absorption limit has a much higher probability of absorption by the transition from the K-shell into the continuum than from the L-shell or even higher lying shells. These facts can clearly be seen in Fig. 6, which demonstrates the relationship between absorption and emission spectra in the X-ray region. The absorption coefficient μ_{abs} between the absorption edges decays according to $\mu_{abs} \sim Z^x/(h\nu)^3$, with

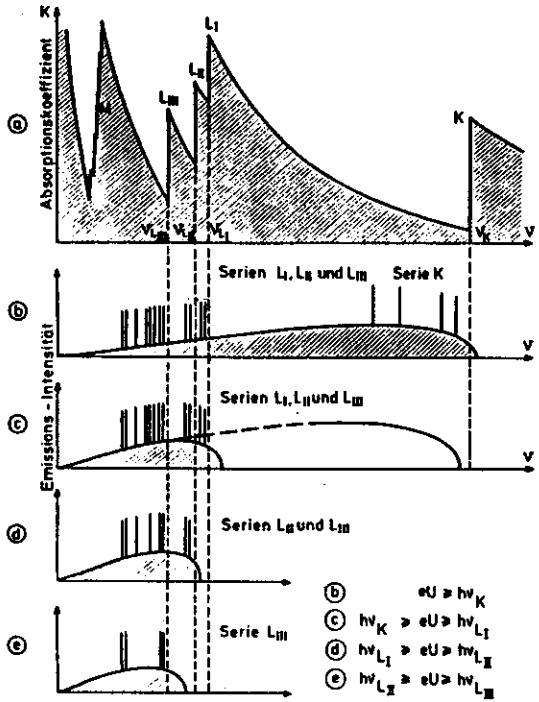

Fig. 6

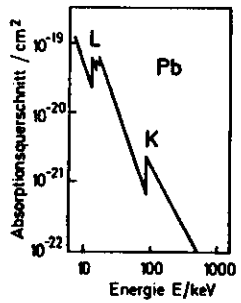

Fig. 7

$3 \leq x \leq 4$, Z the atomic number, and hν the quantum energy, or $\mu_{abs} \sim \lambda^3 Z^x$. This behaviour is shown in a double-logarithmic plot for Pb (Z = 82) in Fig. 7.

Not all excited atoms (i.e. atoms with a vacancy in an inner shell) decay by emission of X-ray radiation. A mechanism for radiationless deactivation is the Auger-effect or inner photo-effect. In the case of a vacancy in, say, the K-shell, the energy of the transition from the L-shell to the K-shell is used for the promotion of another electron of the L-shell into the ionization continuum (with a certain amount of excess energy which appears as kinetic energy of the Auger-electron). This is schematically depicted in Fig. 8. The quantum yield for the emission of X-ray radiation is defined by

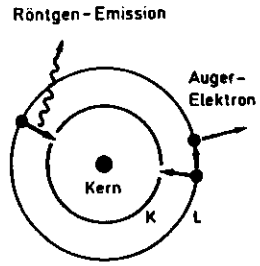

Fig. 8

$$\eta = \frac{\text{number of emitted quanta}}{\text{number of atoms ionized in the particular shell}}$$

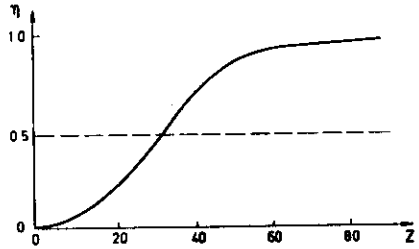

Figure 9 gives η as a function of Z and is of great importance for the pumping of X-ray lasers.

Fig. 9

3. Some X-Ray Laser Mechanisms

A selection of the most promising X-ray laser mechanisms are presented here, following closely ref. 2. A more complete account of other mechanisms can be found in ref. 3.

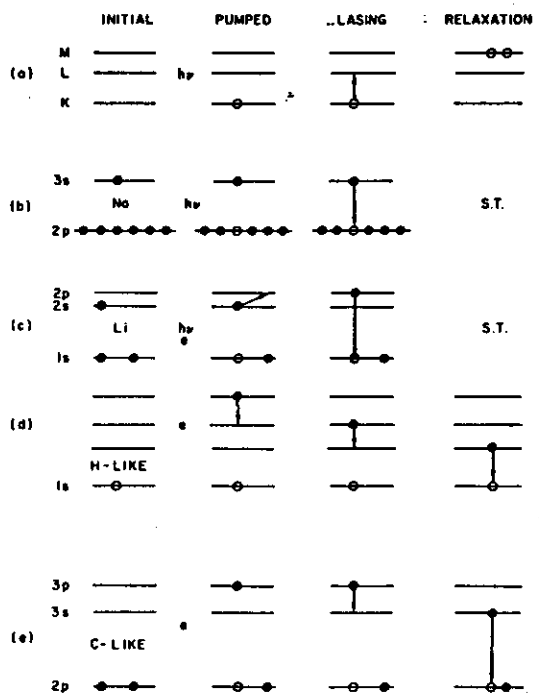

Fig. 10

Figure 10 is an overview of these schemes, showing first the initial state, second the pumped state with the pumping mechanism (hν means pumping by another X-ray quantum, e means pumping by electron collisions) third the lasing transition, and fourth the relaxation mechanism of the lower laser level or the indication that there is none and consequently the laser self-terminating (S.T.).

The first mechanism shown (Fig. 10a) is an inner shell scheme. Here initially all shells shown are filled, which could either be indicated by putting on the lines indicating the K, L, M levels as many filled circles as there are electrons or, as done here, indicating that there are no vacancies (or "holes"), by not putting any symbol on the lines. Pumping by an X-ray quantum of shorter wavelength than the K-edge will then create a vacancy in the K-shell as indicated by the "hole"-symbol on the K-line. Lasing can then occur by filling the vacancy with an electron from the L-shell, which means a jump of the hole from the K- to the L-shell. Now the hole is sitting on the L-shell and can be filled by absorption of an X-ray quantum of exactly the wavelength of the lasing transition, which might constitute a serious reabsorption loss. This loss can be avoided if the L-vacancy is filled either by a radiative transition of an electron from M- to L-shell or radiationless transition by an Auger-transition creating two M-vacancies. Since the radiative lifetime of the lower laser level is longer than that of the upper laser level, a purely radiative relaxation cannot prevent accumulation of vacancies on the L-shell after a short period of lasing, thus destroying the inversion. Self-termination can only be avoided by a sufficient shortening of the lower-state lifetime by a radiationless Auger transition. One might wonder whether the radiationless Auger transitions filling up a K-vacancy by creating two L-vacancies might not constitute a serious loss factor preventing laser action by increased reabsorption especially in low-Z elements with their high Auger coefficient. This is not the case, since the resulting absorption line is shifted considerably by the reduced electronic interaction (e.g. in the case of the Cu-K_α line about 50 eV). This K-shell pumping scheme requires a powerful pump source which must selectively pump the K-shell without significantly disturbing the outer shells.

The next inner-shell scheme (Fig. 10b) although avoiding complications by Auger transitions, is self-terminating, i.e. allowing lasing only for a short time (0.4 ns in the case of

Na, depicted here). It is based on a 3s-2p transiton in Na atoms or Na-like ions (37 nm in the case of Na and correspondingly shorter in Na-like ions). There are no Auger transitions because the lasing transition involves the outermost electron.

The next scheme (Fig. 10c) is also an inner-shell scheme, but implies the use of a metastable level. In the case of Li (or Li-like ions) shown here, the pump radiation removes a 1s-electron thus creating a metastable state. If simultaneous electron collisions or intense long wavelength radiation transfer the 2s-electron to the 2p-level at a rate faster than the decay rate of that level, inversion is created for strongly allowed 2p-1s lasing transition. The metastable state might also be created in a plasma afterglow. Again, the lasing transition is obviously self-terminating.

The scheme of Fig. 10d is an outer-shell scheme that makes use of the recombination of electrons in a rapidly cooling plasma with highly-stripped ions, e.g. hydrogen-like ions as shown here. The electrons could either be free electrons or captured by charge-transfer from another atom or ion in a collision. Since the lower states decay more rapidly than the upper lasing level, one can even expect quasi-cw operation.

The scheme of Fig. 10e depicts the extrapolation of the usual ion-laser scheme of np-ns lasing transitions (e.g. Ar^+ laser: 4p-4s) to shorter wavelengths in highly-stripped ions. The pumping mechanism could be collisional excitation or ionization followed by recombination and reionization.

4. The Pump Power Problem

When considering the threshold pump power of an X-ray laser one must realize that the surface reflectivities of all materials rapidly tend towards zero with decreasing wavelength in the VUV region, so that no resonators can be built, which would store inversion and thus alleviate the pump power problem. Even though considerable progress has been made in making multilayer reflectors for the VUV, reaching 20 to 50 % reflectivity in narrow spectral regions, one cannot expect these lossy coatings to be able to withstand the high expected intensities in an X-ray laser resonator. Presently the only hope is an ASE-device (ASE = amplified spontaneous emission). If we consider a rod-like structure of diameter d and length L, it would emit with a beam divergence of the aspect ratio d/L. If this ratio equals the diffraction limit λ/d, the output will be coherent. The optimum diameter is thus $d = \sqrt{\lambda \cdot L}$. A smaller diameter will lead to diffraction losses.

We can define threshold for such a device so that a photon released spontaneously on one end of the rod just stimulates another photon at the other end. This means $\sigma \cdot N^* \cdot L = 1$, where σ is the stimulated cross-section of the transition used and N^* is the inversion. According to general consensus one could only speak of a laser when an amplification of 1000 has been reached, i.e. $\exp(\sigma N^* L) > 1000$. Since the cross-section σ_m at line center can be calculated as $\sigma_m = \lambda^2/(4\pi^2 \cdot \Delta\nu \cdot \tau_r)$, where $\Delta\nu$ is the linewidth and τ_r is the radiative lifetime of the transition, one can determine the necessary inversion N^* for a given pumped length, provided that linewidth and radiative lifetime of the transition is known. To give an example, we choose the copper $K_{\alpha 1}$-line (K-L_3). Here $h\nu = 8$ keV, $\lambda = 1.54$ Å, $\Delta\nu = 5 \cdot 10^{14}$ Hz, $\tau_r = 1.5$ fs, resulting in $\sigma_m = 8 \cdot 10^{-18}$ cm^2.

With $\exp(\sigma_m N^* \cdot L) > 1000$ rewritten as $N^* > \ln 1000/(\sigma_m \cdot L)$ and assuming $L = 5$ mm, we obtain $N^* > 1.73 \cdot 10^{18}$ cm^{-3}.

To find the minimum pump power, we assume the optimum diameter d of the rod: $d = \sqrt{\lambda \cdot L} \approx 1$ µm (forgetting for the moment the technical difficulties of realization of such a tiny target). The total number of excited copper ions then is $n_t = N^* \cdot \pi \cdot d^2 \cdot L/4$ and with the actual lifetime, $\tau = 0.45$ fs, the power necessary for maintaining this inversion is $P = n_t \cdot h\nu/\tau = 0.26$ TW. Since the power scales as d^2, a fiber of 10 µm diameter would already need a minimum pump power of 26 TW.

More interesting is the minimum power flux that is needed. Assuming again the 1 µm fiber with a surface $A = 1.6 \cdot 10^{-4}$ cm^2 the flux is $W = P/A = 1.6 \cdot 10^{15}$ W/cm^2, and in the case of the 10 µm fiber, we have $W = 1.6 \cdot 10^{16}$ W/cm^2. Even higher power, of course, will be required to reach threshold because of unavoidable inefficiencies.

These power densities can actually be reached today with either of three means:

1. lasers,
2. particle beams,
3. nuclear explosions.

Here we are only concerned with the first possibility.

4. Laser-Generated Plasmas

A laser-generated plasma can serve a triple purpose: 1. generate X-ray emission in various ways, which can be used as pump radiation for inner-shell schemes, 2. generate highly-stripped ions for outer-shell schemes, and 3. supply a high-density pool of electrons, which are needed in various excitation and relaxation processes, as explained before.

How is the process of plasma generation started by a laser beam? Let us again assume a 1 TW peak power laser beam focussed on a fiber with 10 µm diameter and 5 mm length. The intensity is then $I_p \approx 6.4 \cdot 10^{14}$ W/cm^2. The corresponding electric field strength E_p can be calculated as

$$E_p/(\mathrm{V/cm}) = 27.4\sqrt{I_p/(\mathrm{W/cm^2})} \approx 7 \cdot 10^8 \text{ V/cm} = 7 \text{ V/Å}.$$

Since such a field strength is comparable to the field strength in the outermost shells of atoms, field-ionization can set in. The electrons thus created are strongly accelerated by the high electric field in the focussed beam and are then able to ionize further atoms and ions in collisions. In this way very quickly a high-density plasma is created.

What are the interaction mechanisms between a high-intensity laser beam and a high-density plasma? The answer to this question is different for long laser pulses (several ns pulse duration, or longer) and for short pulses (several ps, or shorter) with an intermediate gradual transition region. In the short-pulse regime we have only to consider two mechanisms: 1. inverse bremsstrahlung, 2. resonance absorption. For the long-pulse regime one has to consider a multitude of additional effects, like stimulated Raman scattering, stimulated Brillouin scattering, two-plasmon instability, and filamentation, to name only a few of the most important.

For the relatively large targets and long pulses of laser fusion work, one must carefully consider all of these effects, which make huge computer-codes mandatory. For X-ray

laser work just the opposite applies. We have seen that one has to use targets of only a few microns diameter and a few mm long, and the very short lifetimes of the upper X-ray laser levels dictate the use of short pulses, if one wants to achieve reasonable efficiencies. We will thus only treat inverse bremsstrahlung and resonance absorption.

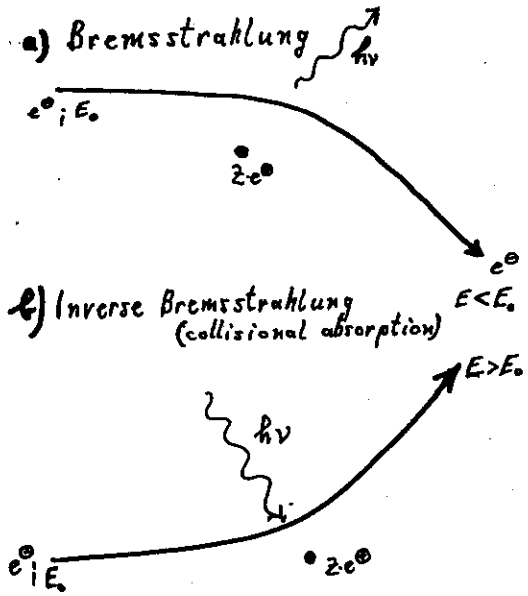

Fig. 11

As the name implies, inverse bremsstrahlung is just the reverse of bremsstrahlung as indicated in Fig. 11. This process is also often referred to as collisional absorption for obvious reasons. The absorption coefficient for this free-free transition is given by (4)

$$k_{ff} = \frac{4.97 g Z^2}{\lambda_L^2 T_e^{3/2}} \cdot \frac{n_e n_i}{n_c},$$

where T_e is the electron temperature in keV, λ_L is the laser wavelength in μm, g is the quantum-mechanical Gaunt factor, which is calculated to be close to unity, n_e and n_i are the density of the electrons and ions, respectively, and n_c is the

critical density to be calculated below. The most important facts to be learned from this formula are the importance of this effect for high-Z targets and the advantage of short laser wavelengths to obtain high absorption. So one sees that a CO_2-laser beam has a 100times lower absorption probability than a Nd-laser beam, and a KrF laser beam again is 18times better absorbed than a Nd-laser.

The critical density n_c of a plasma is that density, beyond which no transverse electromagnetic radiation can propagate. This can be seen from the dispersion relation of a plasma, which is changed from the normal dispersion relationship $k_L^2 \cdot c_o^2 = \omega_L^2 \cdot \varepsilon$ ($\varepsilon = n^2$), with $k_L = 2\pi/\lambda_L$ the wavevector of the laser light, c_o the speed of light in vacuum, ε the dielectric constant and n the refractive index, into the relationship

$$k_L^2 \cdot c_o^2 = \omega_L^2 \left(1 - \omega_p^2/\omega_L^2\right)$$

with $\omega_p = \sqrt{4\pi \cdot n_e \cdot e^2/m_e}$, the plasma frequency (e is the charge and m_e the mass of the electron). It is obvious that k becomes imaginary, when $\omega_L < \omega_p$. This means that all laser light is reflected at a critical electron density n_c that is calculated by letting $\omega_p = \omega_L$ and solving for n_e:

$$n_c = \omega_L^2 \cdot m_e/(4\pi e^2).$$

Here again the advantage of short wavelengths is clearly seen, penetrating to higher electron densities, resulting in higher absorptive path lengths and concomitantly reduced reflective losses.

For resonance absorption to occur, the laser field must interact with a plasma density gradient to produce longitudinal electric waves (plasma or Langmuir oscillations). This can only happen, if the electric vector of the laser light

has a component in the direction of the density gradient of the plasma. Consequently, resonance absorption shows a strong dependence on polarization (only p-polarization, no s-polarization absorbed) and angle of incidence of the laser light, as indicated in Fig. 12 and Fig. 13. Here L is a scale length of the density gradient, assuming a linear rise in electron density from zero to n_c, A is the power absorption coefficient and k_o the vacuum

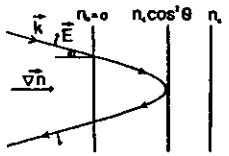

Fig. 12

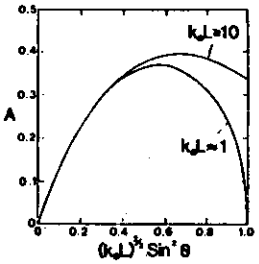

wavenumber. If the angle of incidence θ is very large, then the light is already reflected at the low electron density $n_e(\theta) = n_c \cos^2\theta$ and little light is absorbed; if $\theta = 0$, then $\vec{E}\cdot\vec{\nabla}n_e = 0$ and no light is absorbed. The peaking of the absorption for the

Fig. 13

p-polarization is clearly demonstrated for the experimental results shown in Fig. 14 (5). The laser intensities in this case were in the range from 10^{15} to 10^{16} W/cm^2 and the pulse duration 30 ps from a Nd-glas laser. The in-

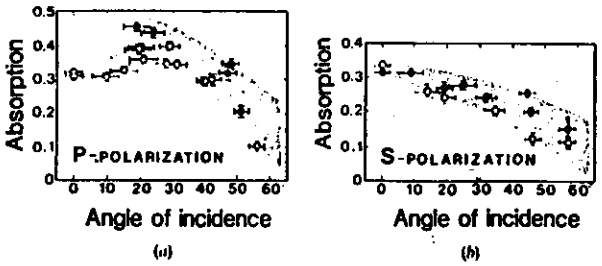

Fig. 14

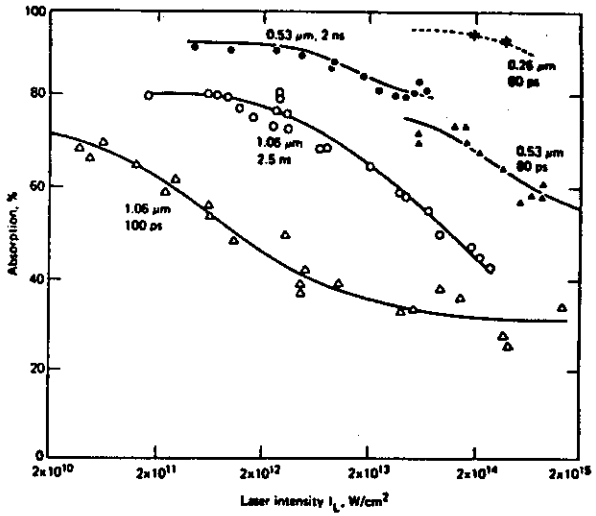

fluence of the wavelength, pulse length and intensity can be seen in Fig. 15, which clearly shows the overwhelming importance of short wavelengths (6).

Fig. 15

5. Experimental Results of X-Ray Laser Work

The many attempts to realize an X-ray laser in the late sixties and early seventies were all unsuccessful (7). The first reliable measurement of gain in a laser-generated plasma at 182 Å was achieved by Pert and coworkers in a series of publications between 1976 and 1982 (8). They used a Nd-glass laser with up to 8 J in 180 ps, focussed, as shown in Fig. 16, in a line 2 mm long and 40 μm wide. In the focal line carbon fibers of 2 to 8 μm

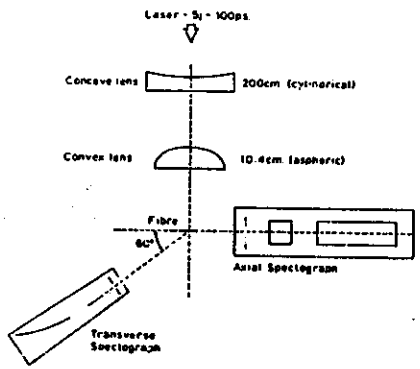

Fig. 16

diameter were located. The output of the C VI (hydrogen-like ion) was analyzed with two calibrated spectrographs, one looking along the axis of the fiber, the other measuring the spontaneous output under 60° to the optical axis. At full laser input energy of 8 J (of which most, of course, was passing by the fiber) a gain-length product of 5 was measured, certainly beyond doubt a significant gain, but still an order of magnitude below the presently accepted definition of an ASE-laser.

After many years without success, it was only an announcement on 29 October, 1984, from a group of 27 researchers from the Lawrence Livermore National Laboratory, headed by Dennis Mathews, that claimed to have achieved laser action in a target of selenium at a wavelength of 206 and 209 Å, measuring an amplification of 700 along the target (9).

They used the lab's giant Novette Nd-glass laser built for fusion work. The pump laser energy of 2 kJ in 450 ps after frequency doubling and focussing resulted in an irradiation intensity of $5 \cdot 10^{13}$ W/cm^2 on the target. This target was a 75 nm thick evaporated strip of Se on a 150 nm thick foil of Formvar. Its length was varied from 11 to 22 mm for the measurement of the gain factor, and it was 0.15 to 0.2 mm wide.

The output was no more than 0.1 µJ, but up to 1 mJ are expected on saturation. The lasing transition was a 3p-3s transition of the neon-like Se-ion (ground state $1s^2 2s^2 2p^6$) that was excited by electron collisions to several $1s^2 2s^2 2p^5 3p$ configurations as upper laser level. The deactivation of the lower laser level is by a fast 3s-2p transition.

Later on an Yb-target showed similar gain on a 155 Å transition. There is good reason to expect lasing in Mg at 13 nm and Mo at 10 nm.

6. Developmental Trends

There is no doubt that the success at LLNL will spur other groups to higher activities. One possibility for progress is the availability in the near future of powerful ps-excimer lasers, especially KrF lasers. A first report on X-ray emission from KrF laser-produced Al plasmas (10) is raising hopes, even though in this case a pulse duration of 50 ns was still used. The use of ps- or even fs-pulses, a travelling wave excitation, and much improved focussing optics (11) might make X-ray lasers possible, which are similar to that of LLNL, but with pump pulse energies that are smaller by a factor of 2000. An additional topic that leaves much room for improvement is the design of multilayered targets for inner-shell excitation schemes, e.g. an inner lasing material coated by a filter material to discard the softer X-rays and permitting only to pass the hard X-rays created in the outermost target layer. Theoretical work covering the plasma generation in the regime of subpicosecond pulses at the extreme irradiation intensities that will become available in the near future, and about which virtually nothing is known, will certainly stimulate new experiments. We can, after all, look forward to an exciting future in X-ray lasers.

References

1. X-Ray Microscopy, Editors G. Schmal and D. Rudolph, Springer-Verlag, Berlin etc., 1984
2. R. C. Elton: X-Ray Lasers, in: Handbook of Laser Science and Technology, Ed.: M. J. Weber, CRC Press, Inc., Boca Raton, Florida, 1982
3. R. W. Waynant and R. C. Elton: Review of Short Wavelength Laser Research, Proc. IEEE 64 (1976) 1059 - 1092
4. K. A. Brückner and S. Jorna: Laser driven fusion, Rev. Mod. Phys. 46 (1974) 325
5. E. T. Kennedy: Plasma and intense laser light, Comtemp. Phys. 25 (1984) 31 - 58
6. T. H. Johnson: Inertial Confinement Fusion: Review and Perspective, Proc. IEEE 72 (1984) 548 - 594
7. X-ray lasers: a status report, Editorial in Laser Focus, November 1973, pp. 41 - 46
8. G. J. Pert: XUV and X-ray lasers, in "Lasers - Physics, Systems and Techniques", Ed. W. J. Firth and R. G. Harrison, Proc. of the Twenty-third Scottish Universities Summer School in Physics, Edinburgh, Aug. 1982, pp. 327 - 345, SUSSP Publications, Edinburgh University Physics Dept., King's Buildings, Mayfield Road, Edinburgh.
9. A. L. Robinson: Soft X-ray laser at Lawrence Livermore Lab, Science 226 (1984) 821 - 822
10. Y. Matsumoto, M. J. Shaw, F. O'Neill, J. P. Partanen, M. H. Key, R. Eason, I. N. Ross, Appl. Phys. Lett. 46 (1985) 28 - 30
11. F. P. Schäfer, German Patent application, 1984